Use of a Photoactive Derivative of Actinomycin To Investigate Shuffling between Binding Sites on DNA†

Christian Bailly,‡,§ David E. Graves,‖ Gareth Ridge,‡ and Michael J. Waring*,‡

Department of Pharmacology, University of Cambridge, Tennis Court Road, CB2 1QJ Cambridge, U.K., and Department of Chemistry, University of Mississippi, University, Mississippi 38677

Received February 23, 1994; Revised Manuscript Received May 3, 1994®

ABSTRACT: A photoreactive analog of actinomycin (7-azidoactinomycin D) has been used in experiments to probe directly the shuffling hypothesis of Fox and Waring [Fox, K. R., & Waring, M. J. (1984) *Nucleic Acids Res. 12*, 9271–9285]. According to this theory, actinomycin D molecules initially interact with non-sequence-specific sites on DNA and subsequently "shuffle" along the polymer in a one-dimensional migratory fashion so as to locate their preferred sequence-dependent binding sites. In the study presented here, the drug–DNA complex was allowed to equilibrate (in the dark) for various periods of time, followed by photolysis which renders the complex irreversible and traps the ligand at its instantaneous binding sites. Visualization of the piperidine-labile sites and investigation of how the intensity of reaction at each site changes with time can provide direct confirmation of the shuffling hypothesis. The data reveal that actinomycin D does indeed engage in shuffling along the DNA. After only short equilibration times (20 s) actinomycin D is observed to bind to a variety of sites on the DNA, including many which are not regarded as canonical preferred binding sites at equilibrium. However, after longer periods of equilibration the intensity of reaction is shown to drop as a function of time at nonspecific sites, with corresponding increase at sequence-specific sites. In addition, base sequences which flank the intercalation sites can be seen to play a major role in influencing the binding and sequence specificity of actinomycin.

The antitumor antibiotic actinomycin D inhibits transcript elongation, not initiation, by RNA polymerase (Phillips & Crothers, 1986; Straney & Crothers, 1987). DNA binding (Müller & Crothers, 1968; Waring, 1970, 1981) as well as modulation of topoisomerase activities (Trask & Muller, 1988) could provide a basis for the observed inhibition of transcription *in vitro* and *in vivo* (Richardson, 1966; Hyman & Davidson, 1970; Goldberg & Friedman, 1971). The geometry of the actinomycin D–DNA complex has been well characterized by X-ray crystallography and NMR spectroscopy: the phenoxazinone chromophore intercalates between DNA base pairs, leaving the two pentapeptide lactones lying in the minor groove of the double helix (Sobell, 1973; Patel, 1974; Takusagawa et al., 1982, 1984; Reid et al., 1983; Brown et al., 1984; Scott et al., 1988a,b; Zhou et al., 1989; Kamitori & Takusagawa, 1992). The sequence specificity of actinomycin D binding to DNA has also been firmly established by footprinting studies which demonstrated that the drug binds preferentially at 5′-GpC-3′ steps (Lane et al., 1983; Scamrov & Beabealashvilli, 1983; Van Dyke & Dervan, 1983; Van Dyke et al., 1983; Fox & Waring, 1984a; White & Phillips, 1989; Rehfuss et al., 1990; Goodisman et al., 1992; Goodisman & Dabrowiak, 1992).

Recently, we demonstrated that the key molecular element responsible for the recognition of preferred binding sites in natural DNA fragments by actinomycin D is the 2-amino group of guanine which protrudes into the minor groove (Bailly et al., 1993). DNA base sequences which flank the canonical GpC step are highly influential in directing actinomycin D binding (Lane et al., 1987; Huang et al., 1988; Bishop et al., 1991; Waterloh & Fox, 1991; Bailey & Graves, 1993). Using a variety of -XGCY- self-complementary and non-self-complementary oligonucleotide sequences, Chen (1988a,b, 1990) showed that the -TGCA- sequence represents the most favored binding site for actinomycin D. Actinomycin is without doubt one of the most sequence-selective intercalating drugs (Bailly et al., 1992) although it can also engage in contacts with noncanonical sequences such as GG and GT steps (Snyder et al., 1989; Waterloh & Fox, 1992; Bailey & Graves, 1993).

The therapeutic effectiveness of actinomycin D and correlations between thermodynamic/kinetic properties of ligand DNA–interactions and induced biological effects have prompted intensive investigations into the kinetics of binding of actinomycin to DNA. Earlier studies revealed that the antibiotic dissociates very slowly from DNA (Müller & Crothers, 1968). Moreover, complex formation with DNA was shown to be resolvable into multirate processes (Bittman & Blau, 1975; Mirau & Shafer, 1982). The dissociation of actinomycin D from DNA is complex, requiring up to three rate constants (Fox & Waring, 1984b; White & Phillips, 1988; Chen et al., 1993). With homogeneous DNA systems (i.e., synthetic oligo- and polynucleotides), the antibiotic–DNA interactions may be characterized by several slow, unimolecular processes with qualitatively little or no sequence or length dependence in the binding kinetics (Brown & Shafer, 1987). By contrast, the dissociation of the actinomycin–DNA complex formed with heterogeneous (i.e., natural) DNA fragments is a complex function in which the proportions of the various time constants vary according to the input drug/DNA ratio (Fletcher & Fox, 1993). In 1986, the *shuffling hypothesis* was put forward as a model to explain the time-

† This work was supported by grants (to M.J.W.) from the Cancer Research Campaign, the Wellcome Trust, and the Association for International Cancer Research; and (to D.E.G.) from the National Cancer Institute (NIH; CA 41474) and the Elsa U. Pardee Foundation. G.R. acknowledges the support of the H. E. Durham Fund and Glaxo.

* Address correspondence to this author.

‡ University of Cambridge.

§ Permanent address: Institut de Recherches sur le Cancer, INSERM Unité 124, Place de Verdun, 59045 Lille Cedex, France.

‖ University of Mississippi.

® Abstract published in *Advance ACS Abstracts,* June 15, 1994.

0006-2960/94/0433-8736$04.50/0

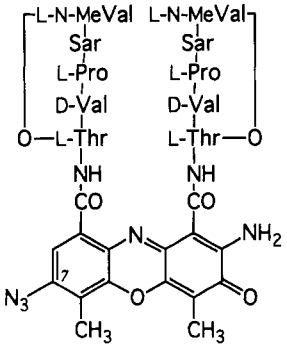

7-Azido-actinomycin

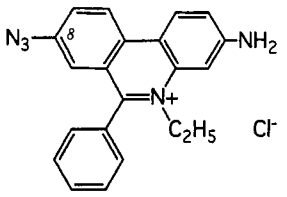

8-Azido-ethidium

FIGURE 1: Structure of 7-azidoactinomycin and azidoethidium chloride. Photolysis of the drug results in the conversion of the azido moiety to a highly reactive nitrene which forms a covalent bond with DNA.

dependent DNase I footprinting patterns observed for actinomycin D–DNA recognition (Fox & Waring, 1986). This theory proposed that molecules of actinomycin D initially bind to relatively nonspecific sites on the DNA and subsequently "shuffle" along the DNA helix to locate preferred binding sites. Although such a process was recently supported by an adaptation of the footprinting experiment to examine the kinetics of dissociation of actinomycin D from different sites (Fletcher & Fox, 1993), the basic hypothesis has never been put directly to the test because of the reversible nature of the interaction between actinomycin D and DNA which renders inconclusive any examination of the kinetics of the DNA-binding reaction alone.

By use of the method of photoaffinity labeling, direct analysis of the postulated shuffling mechanism has now become possible. The photoreactive analog, 7-azidoactinomycin D (Figure 1), has the capacity for covalent attachment to DNA upon photolytic activation and provides a unique probe for an in-depth examination of the time-dependent binding of actinomycin to DNA. Preliminary studies have shown that 7-azidoactinomycin exhibits DNA binding affinity identical to that of the parent antibiotic (Graves & Wadkins, 1989). This photosensitive analog of actinomycin D has also afforded further evidence for the importance of neighboring bases in the binding of actinomycin to GpC sites (Rill et al., 1989). In the present report, we take advantage of the fact that addition of an azido substituent at position 7 converts actinomycin D into an alkylating agent without altering its intercalative DNA binding characteristics, thus allowing us to investigate directly the time dependence of the reaction of 7-azidoactinomycin with a radioactively labeled DNA fragment. Using this strategy, we here demonstrate the shuffling hypothesis to be correct in principle and, in addition, provide further insight into the influence which the base sequence of both the binding site(s) and bases which flank the intercalation sites exert on actinomycin D binding. The experimental approach was to apply the DNase I footprinting technique to locate the regions of DNA covered by the drug coupled with the piperidine-cleavage assay to locate the reactive bases along the DNA lattice.

The data presented here fully support the involvement of a shuffling process in the binding of actinomycin D to natural DNA. In contrast to 8-azidoethidium (8-azido-3-amino-6-phenyl-5-ethylphenanthridinium chloride) (Figure 1), the pattern of binding of 7-azidoactinomycin clearly demonstrates a time-dependent sequence specificity. The results described below lend credence to the hypothesis that actinomycin D moves laterally along the DNA so as to locate its most appropriate binding sites, especially those surrounding GpC dinucleotide steps.

MATERIALS AND METHODS

Chemicals and biochemicals were obtained from the following sources: Ammonium persulfate, Tris base [Tris-(hydroxymethyl)aminomethane], acrylamide, bis(acrylamide), ultrapure urea, boric acid, tetramethylethylenediamine, and dimethyl sulfate were from BDH. Formic acid, piperidine, hydrazine, and formamide were from Aldrich Chemicals, Inc. Developing chemicals were from Kodak. Bromophenol blue and xylene cyanol were from Serva. All chemicals were analytical-grade reagents, and all solutions were prepared by using distilled, deionized, and filtered water from a "Milli-Q" water purification system (Millipore). Calf thymus DNA (highly polymerized sodium salt) was purchased from Sigma Chemical Co., deproteinized with two phenol/chloroform extractions, and then extensively dialyzed against the appropriate buffer. Bovine pancreatic deoxyribonuclease I (DNase, EC 3.1.21.1, Sigma Chemical Co.) was stored as a 7200 units/mL solution in 20 mM NaCl, 2 mM $MgCl_2$, and 2 mM $MnCl_2$, pH 7.3 at −20 °C, and was freshly diluted to the desired concentration immediately prior to use. Restriction endonucleases *Eco*RI and *Pvu*II (Boehringer Mannheim, Germany) were used according to the supplier's recommended protocol in the activity buffer provided. Alkaline phosphatase, AMV reverse transcriptase, and T4 polynucleotide kinase were from Pharmacia. [α-^{32}P]dATP and [γ-^{32}P]ATP (6000 Ci/mmol) were purchased from New England Nuclear. Unlabeled forms of ATP and dATP (ultrapure grade) were purchased from Pharmacia.

Drugs. The initial stock solution was made by dissolving 2 mg of actinomycin D (Sigma Chemical Co.) in 5 mL of water at 4 °C. Ethidium bromide (Aldrich) was first dissolved in water to give a 1 mM stock solution. Subsequent dilutions of the drugs were made with 10 mM Tris and 10 mM NaCl buffer, adjusted to pH 7.0. Drug concentrations were determined photometrically by applying molar extinction coefficients of 25 300 M^{-1} cm^{-1} at 425 nm and 6300 M^{-1} cm^{-1} at 480 nm for actinomycin and ethidium bromide, respectively. 7-Azidoactinomycin and azidoethidium were synthesized according to published procedures (Graves & Wadkins, 1989; Graves et al., 1977). Because of their photosensitivity, the drugs were handled exclusively under photographic safelight conditions. The two photoreactive compounds were dissolved in water (1 mM stock solution), divided into small aliquots, quickly lyophilized, and then stored in sealed 0.5-mL Eppendorf tubes at −70 °C (in the dark). A fresh solution was made each time prior to the reaction with DNA by redissolving an aliquot in buffer to give 1 and 2.5 μM solutions of 7-azidoactinomycin and azidoethidium, respectively.

DNA Purification and Labeling. The plasmid pUC12 was isolated from *Escherichia coli* by a standard sodium dodecyl sulfate–sodium hydroxide lysis procedure and purified by

banding twice in CsCl–ethidium bromide gradients. Ethidium was removed by several 2-propanol extractions followed by exhaustive dialysis against Tris–EDTA buffer. The purified plasmid was then precipitated and resuspended in appropriate buffer prior to digestion by the restriction enzymes. A 178 base pair *Eco*RI/*Pvu*II restriction fragment cut from pUC12 plasmid was used throughout the study. The plasmid was cut with *Eco*RI, treated with alkaline phosphatase, and then labeled at the 5′-end using T4 polynucleotide kinase and [γ-^{32}P]-ATP. The linear labeled plasmid was further digested with *Pvu*II to generate the 5′-labeled fragment. For 3′-end labeling, the plasmid was double digested with *Eco*RI plus *Pvu*II for 3 h at 37 °C and then incubated with AMV reverse transcriptase in the presence of [α-^{32}P]dATP to label specifically the 3′-end at the *Eco*RI site. The singly end-labeled DNA fragment was then purified by preparative nondenaturing polyacrylamide gel electrophoresis (6.5% acrylamide, 1.5 mm thick, 200 V, 2 h, in TBE buffer: 89 mM Tris base, 89 mM boric acid, 2.5 mM Na_2EDTA, pH 8.3). After rapid autoradiography to locate the DNA, the band was excised from the gel, minced with a blade, and extracted overnight in 500 mM ammonium acetate and 10 mM magnesium acetate. The purified DNA was then precipitated twice with 70% ethanol prior to resuspension in 10 mM Tris and 10 mM NaCl buffer, pH 7.0.

DNase I footprinting was performed according to the published protocol (Low et al., 1984), in 10 mM Tris-HCl buffer, pH 7.0, containing 10 mM NaCl, with aliquots removed from the digestion mixture 3 min after the addition of the nuclease. Experiments were performed under safelight conditions to minimize the occurrence of artifacts due to covalent adduct formation. DNase I experiments included approximately 0.02 unit/μL enzyme. The extent of digestion was limited to less than 30% of the starting material so as to minimize the incidence of multiple cuts in any strand ("single-hit" kinetic conditions). Optimal enzyme dilutions were established in preliminary calibration experiments. The reactions were stopped by addition of 3 μL of dye-containing formamide loading buffer. The chemical identities of the digestion products were assigned by coelectrophoresis of sequencing standards generated by treatment of the DNA with dimethyl sulfate (G), formic acid (G+A), or hydrazine (T+C) followed by piperidine-induced cleavage at the modified bases in DNA (Maxam & Gilbert, 1980).

Reaction of 7-Azidoactinomycin with DNA and Production of Drug-Related Strand Breaks. A freshly prepared 1 μM solution of 7-azidoactinomycin was mixed with either the 3′- or 5′-radiolabeled DNA in a final volume of 10 μL and incubated in the dark for the desired length of time (typically 10 s–60 min). At intervals tubes were placed in ice and covalent adduct formation was induced by illumination with a 100-W bulb at a distance of 2 cm from the top of the opened 0.5-mL Eppendorf tube. Illumination was performed for 5 min at 4 °C in order to allow complete covalent DNA adduct formation and to convert the remaining unbound 7-azidoactinomycin into unreactive hydroxylamine species. Control experiments were performed in the absence of drug as well as in the presence of light-inactivated drug (i.e., drug sample light-irradiated for 5 min at 4 °C) to ascertain that the cleavage products effectively result from drug binding and are not due to either spontaneous or light- or heat-induced degradation of the DNA (see Results). Following photolysis, 5 μL of a 1 mM solution of calf thymus DNA was added to the reaction mixture to prevent any remaining photoactivable drug molecules (if any) from further binding to the labeled DNA fragment. The 15-μL drug–DNA solutions were then freeze-dried in dry ice prior to the piperidine treatment. When all tubes corresponding to different incubation times were in dry ice, the DNA samples were mixed with 25 μL of freshly diluted 0.5 M piperidine and heated at 90 °C for 7 min. After freeze-drying, samples were lyophilized repeatedly (up to 4 washes with 50 μL of deionized water) to remove all traces of piperidine salts. Dried samples were finally resuspended in 5 μL of 80% formamide containing 10 mM EDTA and 0.1% bromophenol blue–xylene cyanol as tracking dyes. Samples were heated to 90 °C for 4 min and then chilled in an ice bath just before being loaded on a sequencing gel.

It must be noted that in preliminary experiments we were careful to optimize drug concentration, piperidine concentration, and the heating step in order to visualize the time dependence of DNA strand breakage produced by 7-azidoactinomycin. Drug concentrations that were too high ($\geq$2 μM) did not allow the binding reaction to be monitored. High piperidine concentrations (e.g., 1 M) or longer heating (e.g., $\geq$15 min) resulted in production of degraded DNA samples. The standardized protocol described above was routinely employed and gave reproducible results.

Electrophoresis and Autoradiography. Cleavage products resulting from the DNase I and the photolysis reactions were resolved by polyacrylamide gel electrophoresis under denaturing conditions (0.3 mm thick, 8% acrylamide containing 8 M urea) capable of resolving DNA fragments differing in length by one nucleotide. Electrophoresis was continued until the bromophenol blue marker had run out of the gel (about 2.5 h at 60 W, 1600 V in TBE buffer, BRL sequencers, Model S2). Gels were soaked in 10% acetic acid for 15 min, transferred to Whatman 3MM paper, dried under vacuum at 80 °C, and subjected to autoradiography at –70 °C with an intensifying screen. Exposure times of the X-ray films (FUJI RX) were adjusted according to the number of counts per lane loaded on each individual gel (usually 24 h).

Densitometry and Numerical Analysis. Autoradiographs were scanned using a multichannel computer-operated gel scanner at the Medical Research Council Laboratory of Molecular Biology, Cambridge, by kind permission of Sir Aaron Klug and Dr. J. M. Smith. Gel profiles were plotted and displayed on a raster graphics screen. Quantitative analysis of the gel electrophoresis profiles was limited to regions where peaks were sufficiently resolved to permit accurate analysis and was performed by integration of the area under each peak, using a computer program developed specially for the purpose (Smith & Thomas, 1990). The area under each peak was integrated by simple addition of the pixels under the curve. Footprinting data are presented in the form $\ln(f_a) - \ln(f_c)$ representing the differential cleavage at each bond relative to that in the control (f_a is the fractional cleavage at any bond in the presence of the drug and f_c is the fractional cleavage of the same bond in the control). The results are displayed on a logarithmic scale for the sake of convenience; positive values indicate enhanced cleavage whereas negative values indicate blockage.

RESULTS

DNase I footprinting was carried out on a 178 base pair long restriction fragment obtained by digestion of the plasmid pUC12 with *Eco*RI and *Pvu*II. A typical autoradiogram of a DNase I footprinting assay using the 3′-end-labeled strand of the DNA fragment is shown in Figure 2. Similar gels were obtained with the 5′-end-labeled complementary strand. It is immediately apparent that both actinomycin D and its azido

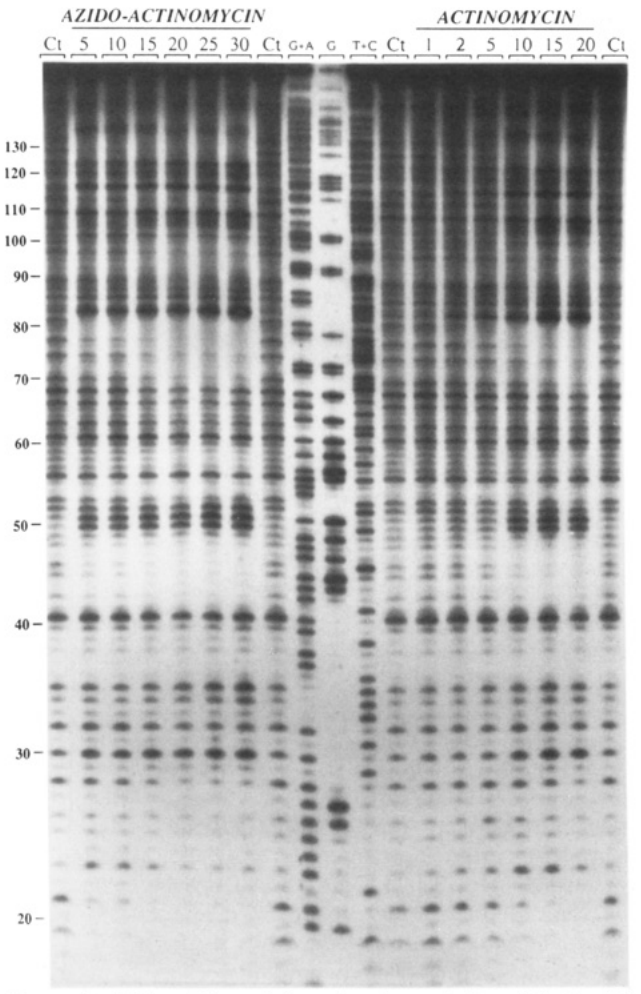

FIGURE 2: DNase I footprinting of actinomycin D and its 7-azido analog on the 178 base pair *Eco*RI/*Pvu*II restriction fragment cut out from plasmid pUC12. The duplex DNA was 3′-end-labeled at the *Eco*RI site with [α-^{32}P]dATP in the presence of AMV reverse transcriptase. The cleavage products of the DNase I digestion were resolved on an 8% polyacrylamide gel containing 8 M urea. The concentration (μM) of the drugs is shown at the top of the appropriate gel lanes. Control tracks labeled "Ct" contained no drug. Tracks labeled G and G+A represent dimethyl sulfate– and formic acid–piperidine markers specific for guanines and purines, respectively. Numbers at the side of the gels refer to the numbering scheme used in Figure 3.

derivative bind preferentially to defined nucleotide sequences in the DNA as judged from the presence of several footprints on the autoradiogram. Clear regions of protection from enzymic DNA cleavage are observed around positions 20, 45, 58, and 75. Dose-dependent enhancement of the cleavage rate relative to that in drug-free control lanes occurs at sequences flanking certain binding sites. Similar concentrations of actinomycin and 7-azidoactinomycin are required to produce the footprints, as expected if the two drugs have similar affinities for DNA. In order to afford a better comparison of the binding specificity of actinomycin and its photosensitive analog, intensities from selected gel lanes were measured by densitometry and converted to numerical probabilities of cleavage.

The differential cleavage plots for the two drugs are superimposed in Figure 3. A portion of about 90 base pairs within the 178-mer was sufficiently well resolved among the different gels scanned to provide quantitative data. Regions of positive differential cleavage (i.e., enhancement) and negative differential (i.e., footprints) are almost completely identical for the two drugs. No significant difference could be discerned between actinomycin and 7-azidoactinomycin. Consistently on both strands of the DNA fragment all sequences protected from DNase I cutting contain a 5′-GpC or a 5′-GpT (ApC) step known to represent the favored binding sites. There are four major protected sites on the 5′-labeled top strand: 5′-GCTGTTTCCTGTGT (19–32, site I), 5′-CGCTCACA (45–52, site II), 5′-ACACAA (58–63, site III), and 5′-CGGAAGCATAA (73–83, site IV). The observed skewing of the footprint pattern to the 3′-side of the binding site arises from the bias introduced by the endonuclease upon DNA cleavage. Taking into account the mechanism of DNase I binding to DNA and in particular the phosphate residues contacted by the enzyme (Weston et al., 1992), it is possible to define with relative accuracy the sites of drug binding. For example, within the sequence

CCGCTCACA
TAGGCGA

(site II) which is protected from cutting by the enzyme, we can predict that in fact the drug is bound to the sequence

CGCT
GCGA

Thus, the DNase I footprinting data provide concrete evidence of the similar sequence selectivity of actinomycin D and azidoactinomycin and endorse the finding that their preferred binding sites are located in GC-rich sites of the DNA.

Photoinduced covalent binding of 7-azidoactinomycin to DNA renders the alkylated bases susceptible to ring opening after treatment with alkali at elevated temperature. The secondary amine piperidine converts the actinomycin-linked base sites into strand breaks. Therefore, using a singly ^{32}P-end-labeled DNA fragment of known sequence, the nucleotide position of the original photoaffinity reaction can be determined by the length of the labeled fragment produced after photoreaction and subsequent piperidine treatment. The same 178 base pair DNA fragment as used in the footprinting assay, either 3′- or 5′-end-labeled, was photoreacted with azidoactinomycin, treated with piperidine, denatured, and electrophoresed. Figure 4 shows the results of such an experiment with the 5′-end-labeled fragment. Under the experimental conditions used, the DNA in the absence of drug remains uncleaved (control lane). In the presence of light-inactivated 7-azidoactinomycin only a subset of cleavage products is visible on the gel (lanes marked *hν*) while with the photoactive 7-azidoactinomycin derivative strong cleavages are detected at various positions in the sequence. The nucleotide sequences that are most sensitive to the drug are all GC-rich. Although drug-related sites of cleavage are predominantly observed at GpC steps, cleavage is not restricted to these canonical sites and can occur at a wide variety of sequences. The autoradiogram shown in Figure 5 displays the results of a kinetic experiment performed with the complementary 3′-end-labeled strand of the 178-mer fragment. Here the time dependence of 7-azidoactinomycin-induced DNA breakage is evaluated over a period of 45 min. The first observation to mention is that the drug reacts very rapidly with DNA; after a 20-s incubation (lane 0.3 min, the shortest time we could examine) multiple and relatively intense cuts were detected all along the DNA sequence. The intensity of the bands varied significantly depending on the sequence targetted, clearly indicating that 7-azidoactinomycin exhibits an initial binding selectivity. For example, the AT-rich sequence between nucleotide positions 30 and 44 is practically unreactive toward 7-azidoactinomycin while the GC-rich sequence from position 45 to 65 is highly sensitive to the drug.

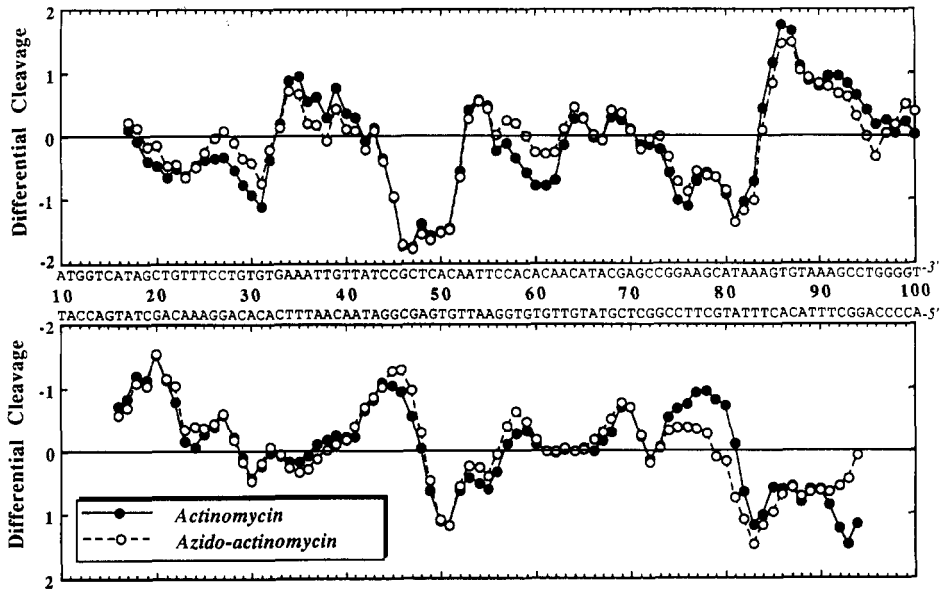

FIGURE 3: Differential cleavage plots comparing the susceptibility of the 178-mer DNA fragment to DNase I cutting in the presence of (●) actinomycin and (○) 7-azidoactinomycin (15 μM each). The upper panel shows differential cleavage of the 5′-end-labeled strand; the lower, that of the complementary 3′-end-labeled strand. The ordinate scales for the two strands are inverted, so that deviation of the points *toward* the lettered sequence (negative values) corresponds to a ligand-protected site and deviation *away* (positive values) represents enhanced cleavage. Vertical scales are in units of $\ln(f_a) - \ln(f_c)$, where f_a is the fractional cleavage at any bond in the presence of the antibiotic and f_c is the fractional cleavage of the same bond in the control, given closely similar extents of overall digestion. Each line drawn represents a 3-bond running average of individual data points, calculated by averaging the value of $\ln(f_a) - \ln(f_c)$ at any bond with those of its two nearest neighbors.

A most interesting observation from this autoradiogram is the time dependence for nucleotide recognition. This is particularly evident at the sequence 3′-AGGCGAGTG (43–51) where significant variations in band intensities are directly observable from the gel. In order to analyze the kinetics of 7-azidoactinomycin binding to DNA on a more quantitative basis, the different lanes on the autoradiogram were densitometrically scanned. Intensities of cleavage (i.e. area under each peak) were expressed in terms of normalized intensity, i.e. the ratio of the intensity of an individual band over the summed intensities of all bands in the corresponding lane. The time dependence of alkylation by 7-azidoactinomycin at each nucleotide through the binding sequence 3′-AGGCGAGT (43–50) is illustrated in the set of cleavage plots shown in Figure 6. Such plots readily permit us to observe movement to and from individual nucleotides within the sequence and provide an overview of the kinetic phenomena which take place at numerous loci within the entire DNA fragment.

The most salient features deduced from these quantitative measurements are the following: (i) plots corresponding to alkylation at the 3′-GpC site (positions 46–47) are characterized by a rapid increase in cleavage intensity. (ii) By contrast, plots for bases situated on the 3′- and 5′-sides of this site (e.g., positions 43–45 and 48) show a more or less steady decrease in cleavage intensity. Therefore, these curves yield unambiguous evidence that the drug molecules initially bind to various nucleotide sequences in a nonspecific manner and over a period of time move to other sites along the DNA helix, hence locating the most favored recognition sites. In other words, these results validate the shuffling hypothesis.

The resolution of the gels proved sufficient to permit accurate analysis of the time dependence of cleavage at 67 nucleotide positions in the DNA (from positions 18 to 84); however, significant time-dependent effects were detected for only a subset of positions (at about 14–18 bases on the two DNA strands). Certain sites, such as the AT-rich regions between positions 30 and 40, showed practically no cleavage even after the longest time of incubation. Other positions were found to exhibit relatively intense cutting but showed little time-dependent variation in intensity (e.g., the cleavage plot corresponding to position 50 in Figure 6), clearly demonstrating that the amplitude of variation in cleavage intensity is highly dependent on the nature of the DNA sequence.

A summary of the DNase I footprints and actinomycin-induced DNA single-strand breakages is presented in Figure 7. A striking observation emerging from these experiments is that nucleotide positions which show time-dependent cleavage are nearly all located within regions of DNA which are protected from DNase I cleavage by actinomycin D. Consistently on both strands of the duplex, the most marked variation in piperidine-sensitive alkylation occurs at the sequence 5′-CGCT (45–48), which also provides the clearest DNase I footprint (site II).

Footprinting and Photoinduced Covalent Binding of Azidoethidium to DNA. In parallel to the actinomycin study, photolabeling experiments were performed with an azido derivative of ethidium bromide (an intercalator generally lacking sequence selectivity) (Figure 1). Both ethidium and 8-azidoethidium failed to yield any clear footprinting pattern with the 178-mer fragment (data not shown). There was little inhibition of DNase I cutting under the experimental conditions used (footprinting was carried out at room temperature). Moreover, no time-dependent cleavage pattern was observed for the covalently bound ethidium–DNA adduct. Figure 8 shows an autoradiogram of a DNA photolabeling reaction conducted in the presence of azidoethidium. As found with 7-azidoactinomycin (Figure 4), light-inactivated azidoethidium produces only a few cleavage products while native azidoethidium alkylates DNA very efficiently. In most instances, the strongest bands generated by azidoethidium photolabeling correspond to guanines and the intensity of those bands does not change with time. The nature of the sequence surrounding each reactive guanosine appears to have no influence on the intensity of the band, in contrast to the results obtained by covalent attachment of 7-azidoactinomycin D. These results are in perfect agreement with previous foot-

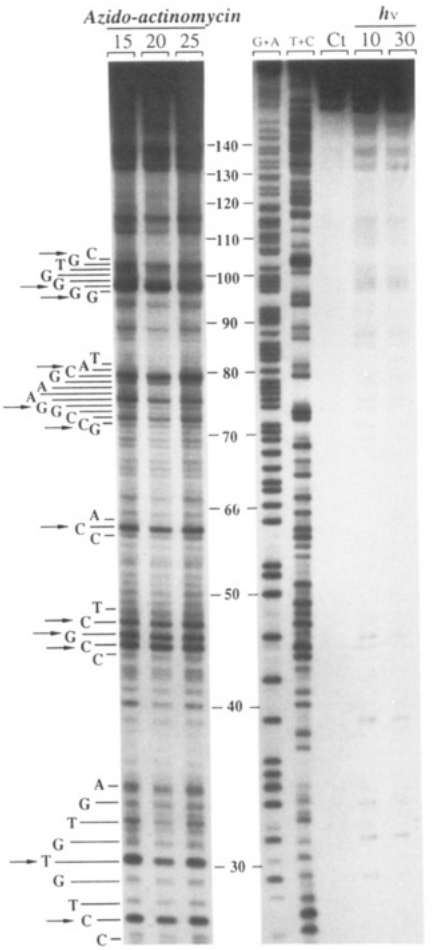

FIGURE 4: DNA photolabeling with 7-azidoactinomycin. The 178-mer DNA fragment labeled at the 5′-end of the *Eco*RI site was reacted with native 7-azidoactinomycin (for 15, 20, and 25 min, left panel) or with light-inactivated ($h\nu$) 7-azidoactinomycin (for 10 and 30 min, right panel) prior to illumination for 5 min at 4 °C. The DNA was subsequently treated with hot piperidine and then electrophoresed on an 8% denaturing polyacrylamide gel. The lane marked "Ct" corresponds to the control DNA subjected to the same treatment in the absence of drug. Purine- and pyrimidine-specific sequence markers obtained by treatment of the DNA with formic acid– and hydrazine–piperidine were run in the lanes marked G+A and T+C, respectively. Numbers between the two panels of the gel refer to the nucleotide sequence of the DNA fragment. A portion of the sequence, identifying the nucleotides with which the azido compound has reacted strongly (indicated by arrows), appears on the left side of the gel.

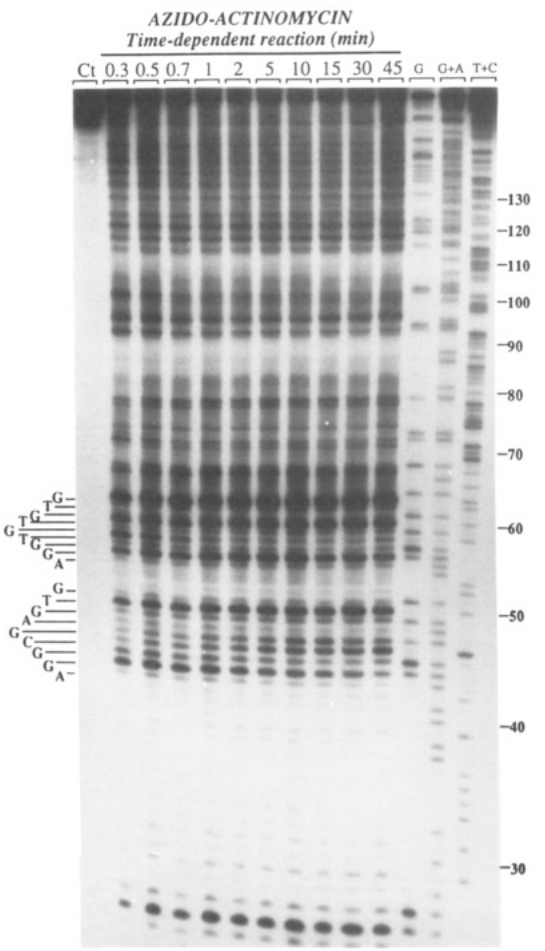

FIGURE 5: Time dependence of the 7-azidoactinomycin-induced DNA strand breakage observed after hot alkaline treatment of the actinomycin–DNA adducts. The 178 base pair restriction fragment labeled at the 3′-end of the *Eco*RI site was incubated in the dark with 7-azidoactinomycin for various lengths of time (0.3–45 min) and subsequently illuminated with visible light to allow adduct formation. DNA molecules were then subjected to piperidine treatment prior to electrophoresis as described in the Materials and Methods. The lane marked "Ct" contained no drug. Lanes marked G, G+A, and T+C are Maxam–Gilbert sequencing standards. Other details as for Figure 4.

printing data (Fox & Waring, 1987) and with other studies on the sequence selectivity of DNA photolabeling with azidoethidium (Marsch, G. A., Graves, D. E., and Rill, R. L., unpublished experiments).

DISCUSSION

The mechanism through which actinomycin D exerts sequence selectivity in binding to DNA has been of paramount interest over the past two decades. Its base-sequence specificity has served as a paradigm in the search for the molecular basis of sequence selectivity of other drug–DNA interactions and has spawned the development of ideas and methods applicable to a range of biologically effective DNA binding agents. The factors which determine the manner in which actinomycin D binds sequence-selectively to DNA remain speculative; however, observations on the complex kinetic data for the association of actinomycin D with DNA led Fox and Waring (1986) to propose the "*shuffling*" model in which the actinomycin is envisaged as initially interacting with DNA in a nonspecific manner, followed by specific redistribution of the antibiotic along the DNA lattice to higher affinity sites. The primary focus of the present study was to probe the validity of the shuffling hypothesis and to seek further information concerning the influence of flanking bases on sequence selectivity. The synthesis of the photoreactive 7-azidoactinomycin D analog provided a probe which has allowed us to examine directly the time-dependent distribution of actinomycin D among different nucleic acid binding sites.

Comparison of Actinomycin D and 7-Azidoactinomycin D Binding to DNA. In order to use photoaffinity labeling as a probe for examining actinomycin D–DNA interactions, it is mandatory to ascertain that prior to photolysis the photoreactive analog binds to DNA in a manner indistinguishable from that of the parent compound. Our footprinting data establish that the base-sequence specificity of the interaction between 7-azidoactinomycin D and DNA appears to be identical to that of the parent actinomycin D. We have further shown that covalent attachment of actinomycin D to DNA does not produce binding artifacts which lead to hypersensitive sites or anomalous cutting regions on the DNA. Preliminary experiments revealed no marked differences between sites at which piperidine-sensitive cleavage of 7-azidoactinomycin

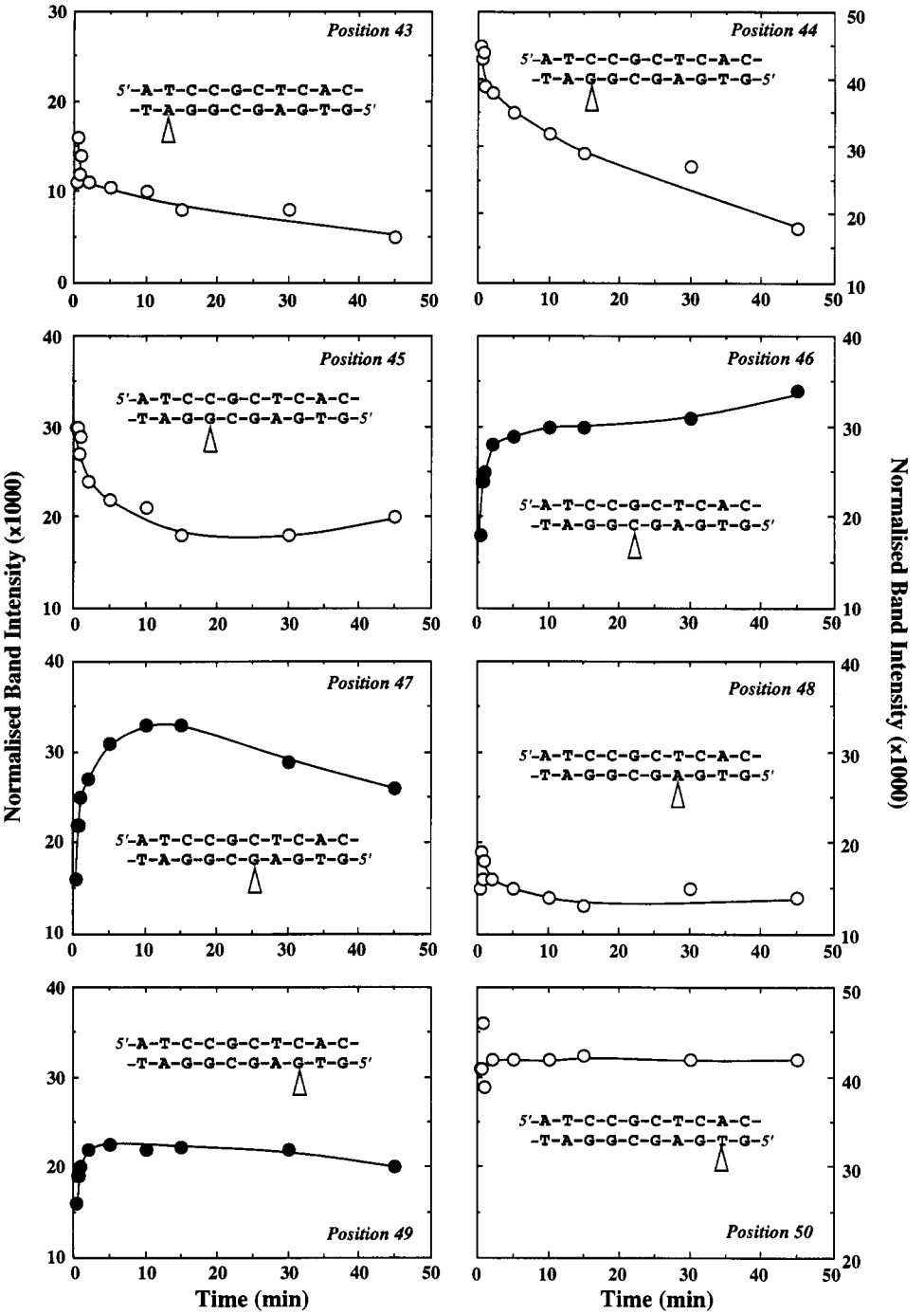

FIGURE 6: Time course of 7-azidoactinomycin-related breaks for selected nucleotides within the DNA sequence 3'-TAGGCGAGTG-5' (42–51). The cleavage plots were obtained after densitometric analysis of the autoradiogram shown in Figure 5. Normalized band intensity refers to the ratio of the intensity of the individual band considered over the total summed intensities of the bands in the same lane. Triangles indicate the nucleotide with which the drug has formed an adduct. Symbols (●) and (○) refer to time-dependent increase and decrease (or no time dependence) in cleavage intensity.

D–DNA adducts could be observed and the classical binding sites of the parent actinomycin D deduced from DNase I footprinting experiments. All of the sites of strand breakage observed with the piperidine cleavage reaction lie within binding sites detected by DNase I footprinting experiments using the nonphotolyzed and photolyzed drug–DNA complexes. As expected, both the regions protected from attack by DNase I and the bonds which become susceptible to cleavage by piperidine are found to be located predominantly at sequences which surround one or more GpC steps.

Exposure of the DNA to intense visible light in the absence of 7-azidoactinomycin D does not result in cleavage. Similarly, DNA exposed to (pre)photolyzed drug inactivated by prior irradiation is cleaved only at a few peculiarly piperidine-labile sites containing guanines (as happens with the same DNA in the presence of the parent actinomycin D). By contrast, adducts formed by photolysis of the 7-azidoactinomycin–DNA complex give rise to marked enhancement of DNA cleavage upon piperidine treatment, allowing us to probe directly the modified sites on the DNA. Using this method, relatively low concentrations of ligand (covalently attached to the DNA) can be used to probe sequence-specific sites on the macromolecule. Experiments with reversible binding ligands such as the parent actinomycin D require much higher concentrations to achieve comparable footprinting resolution. These higher drug concentrations may in fact mask lower affinity

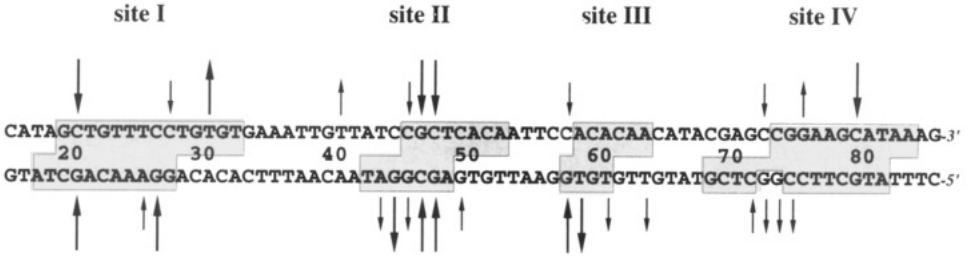

FIGURE 7: Diagrammatic representation of the DNase I footprints and DNA strand cleavages produced by 7-azidoactinomycin on both strands of the 178-mer DNA fragment. Only the region of the restriction fragment which was analyzed by densitometry is shown. The sequences enclosed by gray boxes represent the measured footprints, i.e., positions of inhibition of DNase I cutting by 7-azidoactinomycin, and therefore the putative reversible binding sites. The 3′-offset of the boxes on the two strands of the duplex is in accord with the model for asymmetric DNase I footprinting patterns. Arrows indicate sites of azidoactinomycin-mediated cleavage, with small and large arrows denoting moderate and large variations in the amplitude of the effect with time, respectively. Arrows pointing toward the lettered sequence refer to observed time-dependent increases in cleavage intensity; arrows pointing away from the sequence indicate nucleotides where reactivity diminishes with time of incubation.

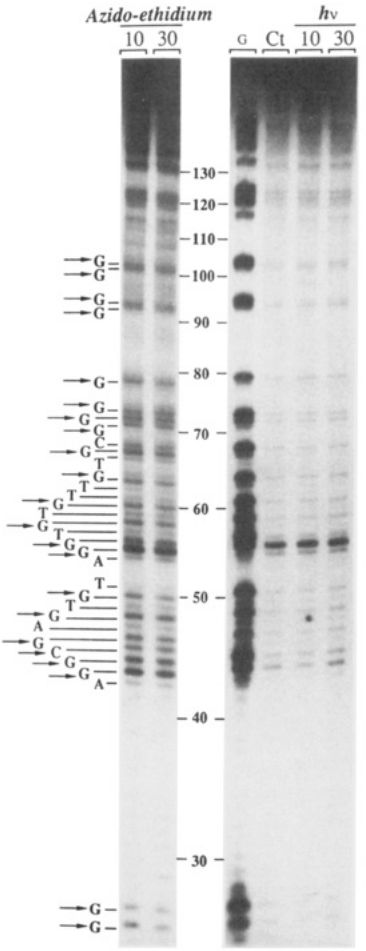

FIGURE 8: DNA photolabeling with azidoethidium. The autoradiogram shows the reaction of native and light-inactivated (*hν*) azidoethidium with the 178 base pair restriction fragment labeled at the 3′-end of the *Eco*RI site. Guanine residues to which azidoethidium is covalently bound upon photolysis are indicated by arrows on the left side of the gel. Other details as for Figure 4. The band at position 55 in the right-hand tracks is spurious, most likely arising as a result of thermal degradation of the original restriction fragment or possibly a contaminant present in it.

sites such as those postulated in the "shuffling" model which are consequently unobservabable using routine DNase I footprinting methodology.

Global Specificity: The First Level of DNA Recognition. Examination of Figure 5 reveals that even at the shortest equilibrium times examined (20 s) the distribution of actinomycin D along the DNA lattice is regionally selective, with the antibiotic virtually absent from sequences having a high AT content, indicating that the initial event in the formation of an actinomycin D–DNA complex may be a first-level recognition of some structural feature like the minor groove geometry. The minor grooves of DNA lattices having high AT content within localized sites are narrower in comparison to other regions of DNA with high GC or mixed sequences (Neidle, 1992; Fox, 1992; Boutonnet et al., 1993). The lack of actinomycin D binding to AT-rich sites, even at early equilibration times, may be indicative of a structural requirement involving the minor groove which is necessary for antibiotic binding. By the same token, DNA regions with GC or mixed sequences having a wider minor groove may be better able to accommodate actinomycin D so that early binding of the antibiotic to these regions is observed. In this context, it is interesting to speculate on the observations of Krugh and Young (1976) who found that, in the presence of low levels of daunorubicin or Adriamycin (1 drug molecule per 10–20 base pairs), actinomycin D could be observed to intercalate into poly(dA-dT). Normally actinomycin does not bind to poly(dA-dT) at all. This enabling phenomenon provoked by simultaneous binding of a relatively nonspecific intercalating antibiotic may reflect structural perturbations within the minor groove induced by the anthracycline–DNA complex which provide a more suitable minor groove geometry for actinomycin D to recognize and associate with.

Non-Sequence-Specific Binding of Actinomycin D to DNA. The present experiments reveal clearly the existence of numerous nonspecific sequences (other than predominantly AT-rich regions) at which actinomycin D can be seen to bind. These interactions are demonstrated to be highly time-dependent, with nonspecific sites dropping in intensity at the same time as preferred sites increase in intensity (here band intensity as determined from densitometric analysis is assumed to provide a direct reflection of drug occupancy, i.e., binding density). At early times (20-s equilibration), actinomycin D is found to interact with a wide variety of sequences other than the classical GpC step. Naturally, the intensity of reaction varies but not much, suggesting that, in regions of the DNA where the minor groove width is accommodating (i.e., non AT-rich regions), binding of actinomycin to DNA occurs in a relatively non-sequence-dependent manner. However, if one focuses on the well-resolved sequence in the 40–50 base pair region, the densitometric analyses presented in Figure 6 reveal that the binding of actinomycin D to such sites is highly time-dependent. Position 47 (GAGCG) represents an initially modest actinomycin D binding site. After 10 min the intensity of this band is enhanced by 2.5 times its initial intensity. However, after 10 min the intensity begins to drop somewhat and by 45 min is down to about 80% of its maximal value. In contrast, the adjacent C at position 46 (GAGCG)

shows an enhancement of intensity which is reached after only 2 min. Then after another 10 min, the intensity begins to increase at a rate nearly identical to the loss of intensity observed for the adjacent site (position 47). Non-GpC sites such as the flanking nucleotides at positions 43–45 show varying degrees of diminishing intensity as a function of increasing equilibration time, clearly consistent with shuffling onto the nearby GpC step. Thus although the initial binding of actinomycin D to the DNA appears to be fairly non-sequence-specific, the relative magnitudes of band intensity reflecting interactions with the G and C sites soon become 2–3 times higher than those observed for neighboring sites containing A and T bases. In addition, the changes in intensity appear to be greatly influenced by the base sequences which flank the intercalation site. In all cases, the nucleotide positions where time-dependent cleavage can be observed are also present as protected sites within the DNase I footprint.

The concomitant decreases and increases in band intensity observed at neighboring nucleotide positions on the sequencing gels are best interpreted as being due to the shuffling of single ligand molecules from nonspecific binding sites to preferred GpC-containing binding sites. It is easiest to envisage this shuffling as the sideways movement, in each case, of a single antibiotic molecule, but we cannot exclude the possibility that a local dissociation and reassociation reaction takes place. Furthermore, although we endeavored to perform the reactions under "single-hit" kinetic conditions, it remains formally possible that some of the observed time-dependent effects might result from simultaneous reaction with two or more azido-actinomycin molecules. For example, the structural changes in DNA caused by the intercalation of one molecule of azidoactinomycin at a preferred site (e.g., at the GpC step 46–47) could inhibit the reaction of a second molecule at an adjacent site (e.g., at the CpC step 43–44). But we believe that any interpretation involving interaction between multiple bound molecules becomes very unlikely if one considers the well-established mechanism of binding of actinomycin to DNA. Intercalation of the phenoxazinone chromophore at a GpC step involves fitting the two cyclic pentapeptides into the minor groove, each extending for two base pairs either side of the intercalation site (Kamitori & Takusagawa, 1992). Given such a configuration, it is difficult to envisage how two antibiotic molecules could be intercalated less than 4 base pairs apart from each other. Steric hindrance between the peptide rings of two closely clustered antibiotic molecules cannot explain why, for instance, the photoreaction of azidoactinomycin with the cytosine residue at position 46 increases while at the same time the reaction with the neighboring guanine residue at position 45 decreases, unless one or another antibiotic molecule is moving—which amounts to shuffling. Accordingly, the only reasonable explanation left to us is that changes in band intensity are indeed due to movement as a result of the redistribution of drug molecules between local sites in the sequence.

DNA Base Sequence: The Second Level of Binding Specificity. The eventual determinants of actinomycin D–DNA binding specificity are most probably specific contacts between the phenoxazinone ring and pentapeptide side chains of the antibiotic with functional groups of the DNA, both within the intercalation site and at bases which flank the sandwiching nucleotide pairs. Optimal binding of actinomycin D (characterized by a long residence time) doubtless relies on the availability and formation of specific hydrogen bonds and van der Waals contacts between the pentapeptide chains and specific functional groups located within the minor groove of the DNA. After the initial association with actinomycin, any lack of suitable contacts within the binding site should result in rapid dissociation of the antibiotic as is known to occur with simpler DNA binding ligands like ethidium (Bresloff & Crothers, 1975; Wakelin & Waring, 1980). But if there exists the possibility of forming favorable sequence-dependent contacts with critical substituents on the base pairs presented into the helical minor groove, such as the 2-amino group of guanine (Bailly et al., 1993), the residence time of the drug would be increased. Indeed, the formation of such hydrogen bonds and van der Waals contacts may actually be required to promote intercalation of the phenoxazinone chromophore. These events are likely to provide the physical basis for the shuffling phenomenon that we have observed.

CONCLUSION

The present results provide strong support for the shuffling hypothesis by showing directly that the location of actinomycin molecules on a DNA lattice, captured by "snapshots" at various times after initial exposure of the DNA to the antibiotic, changes significantly with time. The most obvious changes are associated with increasing antibiotic binding at the canonical preferred (GpC) sites concomitant with diminishing antibiotic presence at flanking sequences, clearly consistent with sideways movement of antibiotic molecules toward the best binding sites. The results also suggest that there are probably two main components to the process whereby actinomycin recognizes and locates its preferred binding sites. In the first step the antibiotic recognizes the minor groove geometry and can only gain access to DNA sequences presenting a suitably wide groove, as is present at GC-containing sequences but not AT-rich tracts. Second, the drug shuffles along the minor groove of the helix so as to locate GpC sites where tight contacts can be established. According to this view the shuffling mechanism proposed ten years ago is validated and apparently corresponds to the successive reading of particular structural elements in the minor groove of the DNA helix by the antibiotic.

ACKNOWLEDGMENT

The authors thank Dean Gentle for his invaluable technical assistance. We are especially grateful to Dr. J. M. Smith and to Sir Aaron Klug of the Medical Research Council Laboratory of Molecular Biology (Cambridge) for providing access to computer facilities.

REFERENCES

Bailey, S. A., Graves, D. E., Rill, R., & Marsch, G. (1993) *Biochemistry 32*, 5881–5887.

Bailly, C., Hénichart, J. P., Colson, P., & Houssier, C. (1992) *J. Mol. Recognit. 5*, 155–171.

Bailly, C., Marchand, C., & Waring M. J. (1993) *J. Am. Chem. Soc. 113*, 3784–3785.

Bishop, K. D., Borer, P. N., Huang, Y. Q., & Lane, M. J. (1991) *Nucleic Acids Res. 19*, 871–875.

Bittman, R., & Blau, L. (1975) *Biochemistry 14*, 2138–2145.

Boutonnet, N., Hui, X., & Zakrzewska, K. (1993) *Biopolymers 33*, 479–490.

Bresloff, J. L., & Crothers, D. M. (1975) *J. Mol. Biol. 95*, 103–123.

Brown, S. C., Mullis, K., Levenson, C., & Shafer, R. H. (1984) *Biochemistry 23*, 403–408.

Chen, F.-M. (1988a) *Biochemistry 27*, 1843–1848.

Chen, F.-M. (1988b) *Biochemistry 27*, 6393–6397.

Chen, F.-M. (1990) *Biochemistry 29*, 7684–7690.

Chen, F.-M., Jones, C. M., & Johnson, Q. L. (1993) *Biochemistry 32*, 5554–5559.
Fletcher, M. C., & Fox, K. R. (1993) *Nucleic Acids Res. 21*, 1339–1344.
Fox, K. R. (1992) *Nucleic Acids Res. 20*, 6487–6493.
Fox, K. R., & Waring, M. J. (1984a) *Nucleic Acids Res. 12*, 9271–9285.
Fox, K. R., & Waring, M. J. (1984b) *Eur. J. Biochem. 145*, 579–586.
Fox, K. R., & Waring, M. J. (1986) *Nucleic Acids Res. 14*, 2001–2014.
Fox, K. R., & Waring, M. J. (1987) *Nucleic Acids Res. 15*, 491–507.
Gilbert, P. L., Graves, D. E., & Chaires, J. B. (1991a) *Biochemistry 30*, 10925–10931.
Gilbert, P. L., Graves, D. E., Britt, M., & Chaires, J. B. (1991b) *Biochemistry 30*, 10932–10937.
Goldberg, I. H., & Friedman, P. A. (1971) *Annu. Rev. Biochem. 40*, 775–810.
Goodisman, J., & Dabrowiak, J. C. (1992) *Biochemistry 31*, 1058–1064.
Goodisman, J., Rehfuss, R., Ward, B., & Dabrowiak, J. C. (1992) *Biochemistry 31*, 1046–1058.
Graves, D. E., & Wadkins, R. M. (1989) *J. Biol. Chem. 264*, 7262–7266.
Graves, D. E., Yielding, L. W., Watkins, C. L., & Yielding, K. L. (1977) *Biochim. Biophys. Acta 479*, 98–104.
Graves, D. E., Watkins, C. L., & Yielding, L. W. (1981) *Biochemistry 20*, 1887–1892.
Huang, Y. Q., Rehfuss, R. P., LaPlante S. R., Boudreau, E., Borer, P. N., & Lane, M. J. (1988) *Nucleic Acids Res. 16*, 11125–11137.
Hyman, R. W., & Davidson, N. (1970) *J. Mol. Biol. 50*, 421–438.
Kamitori, S., & Takusagawa, F. (1992) *J. Mol. Biol. 225*, 445–456.
Lane, M. J., Dabrowiak, J. C., & Vournakis, J. N. (1983) *Proc. Natl. Acad. Sci. U.S.A. 80*, 3260–3264.
Lane, M. J., LaPlante, S. R., Rehfuss, R. P., Borer, P. N., & Cantor, C. R. (1987) *Nucleic Acids Res. 15*, 839–852.
Low, C. M. L., Drew, H. R., & Waring, M. J. (1984) *Nucleic Acids Res. 12*, 4865–4879.
Maxam, A. M., & Gilbert, W. (1980) *Methods Enzymol. 65*, 499–560.
Mirau, P. E., & Shafer, R. H. (1982) *Biochemistry 21*, 2626–2631.
Müller, W., & Crothers, D. M. (1968) *J. Mol. Biol. 35*, 251–290.
Neidle, S. (1992) *FEBS Lett. 298*, 97–99.
Patel, D. J. (1974) *Biochemistry 13*, 2388–2395.
Phillips, D. R., & Crothers, D. M. (1986) *Biochemistry 25*, 7355–7362.
Rehfuss, R., Goodisman, J., & Dabrowiak, J. C. (1990) *Biochemistry 29*, 777–781.
Reid, D. G., Salisbury, S. A., & Williams, D. H. (1983) *Biochemistry 22*, 1377–1385.
Richardson, J. P. (1966) *J. Mol. Biol. 21*, 83–114.
Rill, R. L., Marsch, G. A., & Graves, D. E. (1989) *J. Biomol. Struct. Dyn. 7*, 591–605.
Scamrov, A. V., & Beabealashvilli, R. S. (1983) *FEBS Lett. 164*, 97–101.
Scott, E. V., Jones, R. L., Banvile, D. L., Zon, G., Marzilli, L. G., & Wilson, W. D. (1988a) *Biochemistry 27*, 915–923.
Scott, E. V., Zon, G., Marzilli, L. G., & Wilson, W. D. (1988b) *Biochemistry 27*, 7940–7951.
Smith, J. M., & Thomas, D. J. (1990) *Comput. Appl. Biosci. 6*, 93–99.
Snyder, J. G., Hartman, N. G., Langlois-d'Estantoit, B., Kennard, O., Remeta, D. P., & Breslauer, K. J. (1989) *Proc. Natl. Acad. Sci. U.S.A. 86*, 3968–3972.
Sobell, H. M. (1973) *Prog. Nucleic Acid Res. Mol. Biol. 13*, 153–190.
Straney, D. C., & Crothers, D. M. (1987) *Biochemistry 26*, 1987–1995.
Takusagawa, F., Dabrow, M., Neidle, S., & Berman, H. M. (1982) *Nature 296*, 466–469.
Takusagawa, F., Goldstein, B., Youngster, S., Jones, R., & Berman, H. (1984) *J. Biol. Chem. 259*, 4714–4715.
Trask, D. K., & Muller, M. T. (1988) *Proc. Natl. Acad. Sci. U.S.A. 85*, 1417–1421.
Van Dyke, M. W., & Dervan, P. B. (1983) *Nucleic Acids Res. 11*, 5555–5567.
Van Dyke, M. W., Hertzberg, R. P., & Dervan, P. B. (1983) *Proc. Natl. Acad. Sci. U.S.A. 79*, 5470–5474.
Wakelin, L. P. G., & Waring, M. J. (1980) *J. Mol. Biol. 144*, 183–214.
Waring, M. J. (1970) *J. Mol. Biol. 54*, 247–279.
Waring, M. J. (1981) *Annu. Rev. Biochem. 50*, 159–192.
Waterloh, K., & Fox, K. R. (1991) *J. Biol. Chem. 266*, 6381–6388.
Waterloh, K., & Fox, K. R. (1992) *Biochim. Biophys. Acta 1131*, 300–306.
Weston, S. A., Lahm, A., & Suck, D. (1992) *J. Mol. Biol. 226*, 1237–1256.
White, R. J., & Phillips, D. R. (1988) *Biochemistry 27*, 9122–9132.
White, R. J., & Phillips, D. R. (1989) *Biochemistry 28*, 6259–6269.
Zhou, N., James, T. L., & Shafer R. H. (1989) *Biochemistry 28*, 5231–5239.